27 May 2010, 11:00 am - 11:20 am

Comparison Between Clean Sand Liquefaction Charts Based on Penetration Resistance and Shear Wave Velocity

Ricardo Dobry

Rensselaer Polytechnic Institute, Troy, NY

Fifth International Conference on
Recent Advances in Geotechnical Earthquake Engineering and Soil Dynamics
and Symposium in Honor of Professor I.M. Idriss
May 24-29, 2010 • San Diego, California

COMPARISON BETWEEN CLEAN SAND LIQUEFACTION CHARTS BASED ON PENETRATION RESISTANCE AND SHEAR WAVE VELOCITY

Ricardo Dobry
Rensselaer Polytechnic Institute
Troy, New York, USA

ABSTRACT

A comparison is conducted between clean sand liquefaction charts based, respectively, on normalized point penetration resistance in CPT static cone tests (q_{c1N}) and shear wave velocity (V_{s1}). Examination of the shape of these field-calibrated curves, review of the factors influencing liquefaction resistance in the laboratory, field correlations between q_{c1N} and V_{s1}, and field and laboratory evidence related to some of the factors influencing cone penetration resistance and shear wave velocity in sands, are all used in the discussion. It is concluded that the difference between the shapes of the two charts at the high end may be due - at least partially - to lateral stress effects associated with overconsolidation and preshaking, which are known to increase liquefaction resistance, and specifically to the higher sensitivity of the penetration resistance to the value of the coefficient of lateral stress at rest, K_0.

INTRODUCTION

Almost 40 years ago, Seed and Idriss (1971) proposed a simplified procedure for evaluating liquefaction potential based on the normalized standard penetration resistance of the sand, N_1 (later refined to $(N_1)_{60}$), obtained from field SPT measurements, and calibrated with actual case histories during earthquakes. The procedure has been modified and improved periodically with more case histories, and similar charts have also been calibrated using the normalized static cone penetration resistance, q_{c1N} (Robertson and Wride, 1998), obtained from field CPT measurements. The latest version of these CPT charts for clean sands is shown in Fig. 1 (Idriss and Boulanger, 2004, 2008). The SPT and CPT charts use the same basic approach and share important characteristics; and they have both stood the test of time by showing again and again their predictive power when earthquakes occur. As a result, they still define today's state-of-practice of seismic liquefaction evaluation of saturated sand sites (Youd et al., 2001; Idriss and Boulanger, 2008).

That is, the original vision of the original Simplified Procedure in 1971, which combined the best available research results with actual earthquake field experiences, managed to produce a viable engineering method for the very complex phenomenon of liquefaction. This and subsequent adaptations and developments such as Fig. 1, illustrates why Dr. Idriss has had such a large impact on geotechnical earthquake engineering: by being both a top engineer and a top researcher and always knowing how to combine the best of both worlds for the benefit of engineering practice.

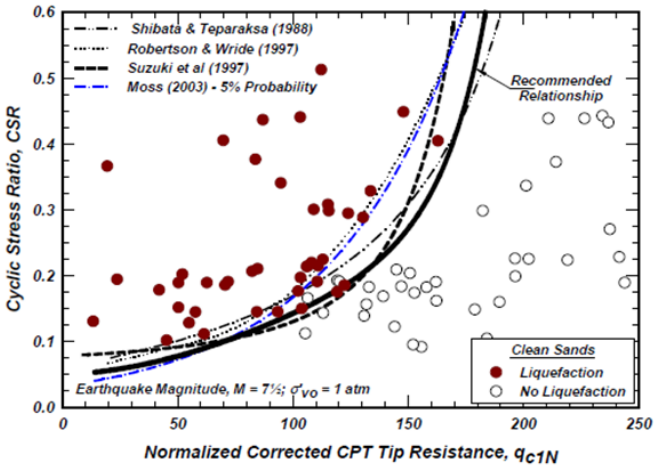

Fig. 1. Liquefaction chart based on point resistance measured during static cone penetration tests, CPT (Idriss and Boulanger, 2004, 2008).

More recently, liquefaction charts have been developed using the same simplified procedure framework, but now based on

the normalized shear wave velocity, V_{s1}, of the sand to measure the liquefaction resistance of the soil. This was originally motivated by the strain approach to liquefaction (Dobry et al., 1981, 1982), and subsequently compared with liquefaction performance at sites in the Imperial Valley earthquakes in Southern California by Bierschwale and Stokoe (1984). A V_s-based liquefaction chart calibrated with a few case histories of liquefaction was proposed by Robertson et al. (1992), and subsequent developments and addition of many other case histories culminated in the Andrus and Stokoe (2000) chart shown in Fig. 2. The chart bounds well the sites that have experienced liquefaction, and thus it has also been added to the arsenal of tools available to practitioners (Youd et al., 2001; Idriss and Boulanger, 2008). Besides the usefulness of Figs. 1 and 2, the fact that both penetration resistance and shear wave velocity - based respectively on field measurements inducing very large and very small strains in the soil - manage to produce liquefaction charts having significant predictive power, makes it worth further comparison and discussion.

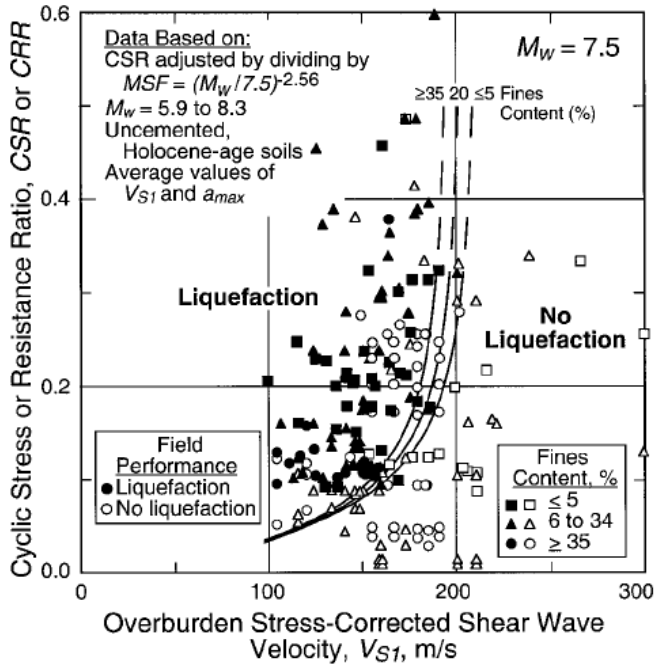

Fig. 2. Liquefaction chart based on measured shear wave velocity (Andrus and Stokoe, 2000).

Idriss and Boulanger (2008) compared liquefaction charts based on penetration resistance and shear wave velocity, such as Figs. 1 and 2. They suggested that greater weight be given to the results of penetration charts, given the higher sensitivity of penetration resistance to changes in the relative density of the sand, D_R. This paper continues the comparison and extends it to other factors in addition to D_R.

The rest of this paper focuses on comparison and observations related to Figs. 1 and 2 for the case of *clean sands* (that is with fines content, FC ≤ 5%). While the CPT chart of Fig. 1 corresponds to clean sands, the V_s chart of Fig. 2 includes both clean and silty sands, so the comparison has to be done with some care. Still, some observations emerge clearly from visual inspection of both figures even when restricting it to sands with FC ≤ 5%:

- The range of values of q_{c1N} for liquefied sand sites corresponds to a factor of about 8 (20-160), compared with a factor of about 2 (100-200 m/s) for V_{s1}, suggesting that q_{c1N} is more sensitive than V_{s1} to the factors underlying the sand liquefaction resistance.
- At the high end of the charts, for which high Cyclic Stress Ratios are needed to trigger liquefaction, the curve in Fig. 1 rises rather smoothly. On the other hand, the curve in Fig. 2 rises abruptly, so that for Cyclic Stress Ratios greater than 0.2, all V_{s1} values are in the extremely narrow range between about 190 and 210 m/s. This again suggests a greater sensitivity of q_{c1N} when compared to V_{s1N}, to the factors underlying sand liquefaction resistance.

DISCUSSION OF LIQUEFACTION CHARTS

Originally it was believed that liquefaction resistance was mainly controlled by either void ratio, e, or relative density, D_R. In that context, penetration resistance (which at that time meant $(N_1)_{60}$), was believed to be mainly or exclusively correlated with D_R. However, first research by Finn et al. (1970), and then several other laboratory cyclic loading studies summarized by Seed (1979) and Finn (1981), showed that a number of other factors could be as important as D_R or e in determining liquefaction resistance. This caused a decisive switch in engineering practice away from the laboratory and toward the use of liquefaction charts based on penetration resistance. In his 1979 paper, Seed proposed as explanation for the success of penetration-based charts, the hypothesis that "the factors tending to increase the resistance to cyclic mobility or liquefaction also tend to increase the penetration resistance of a sand." He listed these factors as: the density or relative density, the grain structure or fabric (method of sand deposition), the length of time the sand is subjected to sustained pressure, overconsolidation and the value of the coefficient of lateral stress at rest, K_0, and preshaking. A recent centrifuge study by Sharp (1999) on a clean sand, has confirmed Seed's hypothesis, showing that both liquefaction and associated ground deformation (lateral spreading, settlement), are better correlated with penetration resistance than with either D_R or e alone when overconsolidation and preshaking are included.

Both overconsolidation and preshaking (Youd and Craven, 1975) increase the value of K_0 of a sand. Overconsolidation and associated increases in lateral stress and K_0 also increase dramatically the values of CPT point resistance and q_{c1N} (Alperstein and Leifer, 1976; Baldi et al., 1981; Lunne and Kleven, 1981; Schmertmann, 1973, 1978). More limited evidence also points to possible large increases in q_{c1N} when

the sand is preshaken with small change in e or D_R (Sharp, 1999). Therefore, while D_R is probably more important at the lower end of the charts, the effect of K_0 may contribute significantly to the success of penetration resistance in predicting liquefaction at the high end, due to the great sensitivity of both liquefaction and penetration resistances to increases in K_0. Therefore, K_0, in conjunction with D_R and perhaps other factors, could explain the overall sensitivity of q_{c1N} to liquefaction resistance, shown by Fig. 1 and discussed in the previous section. The next question is how sensitive is V_{s1} to K_0, as the answer to this may help clarify some of the features of the chart in Fig. 2 discussed in the previous section.

In an effort to understand better the differences between the charts in Figs. 1 and 2, the next two sections discuss, respectively: field-based correlations between q_{c1N} and V_{s1}, and the sensitivity of V_{s1} to K_0 using an available laboratory-based correlation for clean sands.

FIELD CORRELATIONS BETWEEN q_{c1N} AND V_{s1}

Several authors have correlated penetration resistance with shear wave velocity at potentially liquefiable clean sand sites. Youd et al. (2001) presented such a correlation between $(N_1)_{60}$ and V_{s1}, while Andrus et al. (2004) studied the correlation between q_{c1N} and V_{s1} (Fig. 3). These correlations, as well as the additional ones developed by the author and discussed below, are done in two different ways: (i) by using pairs of measurements of q_{c1N} and V_{s1} performed in the same sand layer and depth (data points in Fig. 3); and (ii) by cross-plotting values of q_{c1N} and V_{s1} at the same Cyclic Stress Ratio in liquefaction charts like those in Figs. 1 and 2 (line labeled "curve implied from CRR relationships" in Fig. 3).

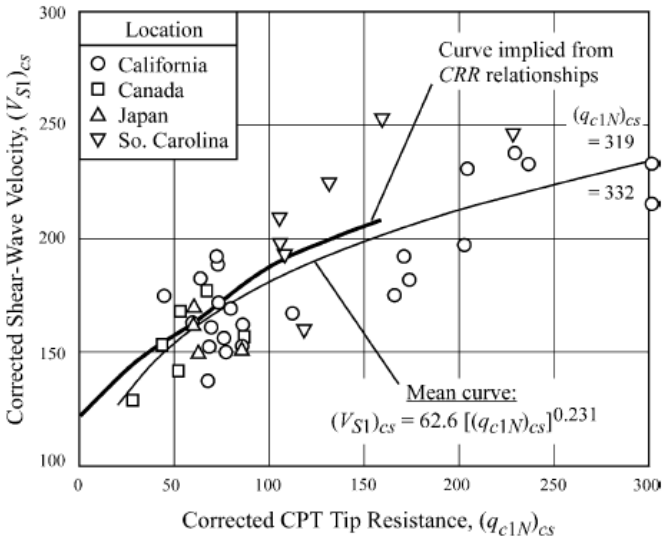

Fig. 3. Field relationships between equivalent clean sand values of q_{c1N} and V_{s1} for uncemented, Holocene sands (Andrus et al., 2004).

The advantage of method (i) is that it is more general and clearly applicable to very liquefiable or very nonliquefiable sands plotting far from the liquefaction-nonliquefaction boundaries in the charts. As illustrated by Fig. 3, the two methods give very similar results, which is encouraging.

However, the mean curve using method (ii) in the figure, of equation:

$$(V_{s1})_{cs} = 62.6\,[(q_{c1N})_{cs}]^{0.231} \quad (1)$$

was obtained by a regression of 39 data points which included silty sands with fines contents up to FC = 20%. For sites with FC > 5%, a correction was applied by Andrus et al. to both V_{s1} and q_{c1N} measurements to obtain "clean sand equivalents," before obtaining the regression equation. To avoid such clean sand correction and to make sure that the regression curve didn't change much when only clean sands were considered, the author repeated the regression using only the 13 sites with FC ≤ 5% included in the database provided by Andrus et al. Both the original Andrus et al. regression and the new regression obtained by the author are listed in Table 1. Furthermore, the "implied" curve in Fig. 3 was obtained by Andrus et al. using q_{c1N} values from the older chart provided by Robertson and Wride (1998). The author recalculated a similar implied regression curve by cross-plotting q_{c1N} and V_{s1} values from Figs. 1 and 2, that is by using the updated CPT curve proposed by Idriss and Boulanger. This new "implied" regression equation between q_{c1N} and V_{s1} is also included in Table 1.

While the three equations listed in Table 1 are different, they predict very similar values of V_{s1} at a given q_{c1N}. For q_{c1N} = 50, representative of the low end of the chart in Fig. 1, the predicted V_{s1} = 148-161 m/s, that is a difference of less than 10%. Similar good agreements within 10% or so are found at the high end of the chart (q_{c1N} = 150), as well as for sites that are definitely nonliquefiable (q_{c1N} = 300). While the information sources used to generate the three equations in Table 1 are limited and overlapping, the agreement is still encouraging.

An important observation about the three regression equations in Table 1 is the fact that the power for q_{c1N} is always much lower than 1.0 (0.15-0.27). This translates into a significant flattening of the curves at higher values of q_{c1N} (Fig. 3), and a decreasing sensitivity there of V_{s1} to large increases in q_{c1N}. As a result, when q_{c1N} increases in Table 1 by a factor of 2 (from q_{c1N} = 150 to 300), the value of V_{s1} increases by only 10-20%. This is consistent of course with the smooth rise of the curve in Fig. 1 and simultaneous abrupt rise of the curve in Fig. 2 at the high end of the chart, already discussed. It suggests again that there is at least one underlying factor controlling liquefaction resistance at the high end of the charts, to which q_{c1N} is much more sensitive than V_{s1}. After the discussion in the previous section, an obvious candidate for the role of such underlying factor, is the effective lateral stress and associated

K_0, which can be increased by either overconsolidation or preshaking.

Table 1. Field correlations between q_{c1N} and V_{s1} (m/s).

Source of Correlation	Sand Description	Equation	V_{s1} (m/s) calculated with Equation for:		
			$q_{c1N} = 50$	$q_{c1N} = 150$	$q_{c1N} = 300$
Andrus et al. (2004) (39 data points, see Fig. 3)	Holocene sand sites with FC ≤ 20% or $I_c \leq 2.25$	$(V_{s1})_{cs} = 62.6\ [(q_{c1N})_{cs}]^{0.231}$	155	199	234
This work, using only those Andrus et al. (2004) sites corresponding to clean sand (13 data points)	Holocene sand sites with FC ≤ 5%	$V_{s1} = 89.3\ (q_{c1N})^{0.150}$	161	189	210
This work, correlating q_{c1N} and V_{s1} from liquefaction – no liquefaction curves in Figs. 1 and 2	FC ≤ 5%	$V_{s1} = 51.1\ (q_{c1N})^{0.272}$	148	200	-

NOTES: FC = fines content; I_c = soil behavior type index obtained from CPT friction resistance; $(q_{c1N})_{cs}$ and $(V_{s1})_{cs}$ = equivalent clean sand values corrected for fines when FC > 5%.

PREDICTED FIELD SHEAR WAVE VELOCITY FROM LABORATORY RESULTS

The author conducted a parametric study to evaluate the sensitivity of V_{s1} to K_0, by using the equation proposed by Hardin and Drnevich (1972) for clean sands (see also Hardin, 1978):

$$G_{max} = 3230\ (2.97 - e)^2\ (\bar{\sigma}_0)^{0.5} / (1 + e) \quad (kPa) \qquad (2)$$

where G_{max} is the shear modulus of the sand at very small strains. The correlation was obtained from a large number of resonant column laboratory measurements in dry sand of G_{max} and $V_s = (G_{max}/\rho)^{0.5}$, where ρ = mass density of the dry soil. In each test the sand specimen of void ratio, e, was confined under an isotropic effective confining pressure, $\bar{\sigma}_0$.

For the parametric study, $V_{s1} = [(G_{max})_1/\rho_{sat}]^{0.5}$, where $(G_{max})_1$ was obtained using Eq. 1 for a vertical effective confining pressure, $\bar{\sigma}_v$ = 1 atmosphere = 101.3 kPa, and ρ_{sat} was calculated for the given void ratio, e, after assuming full saturation with water and a specific gravity of the soil grains of 2.65. Finally, for the field case where the horizontal and vertical effective pressures are usually different, with $\bar{\sigma}_h = K_0\ \bar{\sigma}_v$, $\bar{\sigma}_0$ in Eq. (2) was replaced by the mean effective pressure, that is $\bar{\sigma}_0 = (1 + 2K_0)\ \bar{\sigma}_v/3$. Under these assumptions, the value of V_{s1} is a function of only two parameters, e and K_0. This function is plotted in Fig. 4 for a wide range of possible values of e and K_0, and selected values of V_{s1} have been listed in Table 2.

As additional verification, the author repeated the computations but now using in Eq. (2) the more exact expression for $\bar{\sigma}_0 = (K_0)^{0.5}\ \bar{\sigma}_v$ (Stokoe et al., 1985), instead of the approximation $\bar{\sigma}_0 = (1 + 2K_0)\ \bar{\sigma}_v/3$ utilized to generate Fig. 4 and Table 2. It was found that these two definitions of $\bar{\sigma}_0$ produced values of V_{s1} which were within 2% of each other.

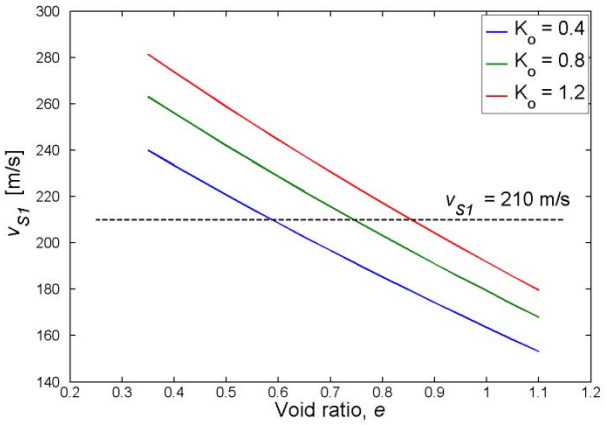

Fig. 4. Normalized shear wave velocity of saturated clean sand, V_{s1}, predicted from the laboratory correlation proposed by Hardin and Drnevich (1972).

Table 2. Values of V_{s1} (m/s) computed using laboratory-based Eq. (2), proposed by Hardin and Drnevich (1972) for clean sands.

Coefficient of lateral stress at rest, K_0	Void ratio, e		
	e = 0.35	e = 0.75	e = 1.1
$K_0 = 0.4$	240	191	153
$K_0 = 0.8$	263	209	168
$K_0 = 1.2$	281	224	180

As expected, Fig. 4 and Table 2 show a significant influence of the void ratio on V_{s1}. For example, for $K_0 = 0.4$, close to the situation expected for a normally consolidated sand, V_{s1} ranges from 153 m/s for very loose sands to 240 m/s for very dense sands. On the other hand, while V_{s1} does increase when K_0 increases, V_{s1} is much less sensitive to this parameter. The total variation in V_{s1} when going from a low $K_0 = 0.4$ to the large $K_0 = 1.2$ that may exist in a heavily overconsolidated sand, is less than 20%. This confirms the assumption that the relative insensitivity of V_{s1} to significant increases in K_0 due to overconsolidation or preshaking may constitute a significant part of the explanation of the shape of the liquefaction chart in Fig. 2 when V_{s1} approaches values on the order of 200 m/s. This is in contrast with the much greater sensitivity of CPT measurements to K_0, which may help explain the smoother shape of the curve at high q_{c1N} in Fig. 1.

The value $V_{s1} = 210$ m/s, which appears to be a limiting value for clean sand liquefaction, at least for the earthquake magnitude associated with Fig. 2 (M = 7.5), has also been superimposed on Fig. 4. While Fig. 4 does not provide an obvious explanation of this limiting V_{s1}, a study of combinations of e and K_0 that produce V_{s1} above and below 210 m/s, may perhaps be a good starting point for future investigations explaining why clean sands in the field don't seem to liquefy when V_{s1} exceeds 210 m/s.

CONCLUSION

A comparison is conducted between clean sand liquefaction charts based on normalized penetration resistance (q_{c1N}) and shear wave velocity (V_{s1}). It is concluded that the difference between the shapes of the two charts at the high end may be due - at least partially - to lateral stress effects, specifically to the higher sensitivity of the penetration resistance to the value of K_0.

ACKNOWLEDGMENTS

The author is grateful to Mr. Vicente Mercado for his help in the computations, and to him, Ms. Victoria Bennett and Dr. Michael Sharp for their helpful suggestions after reviewing the paper.

REFERENCES

Alperstein, R., and Leifer, S.A. [1976]. "Site Investigation with Static Cone Penetrometer," *ASCE J. of the Geotech. Eng. Div.*, 102(GT5), 539-555, May.

Andrus, R. D., and Stokoe II, K. H. [2000]. "Liquefaction Resistance of Soils from Shear Wave Velocity," *J. Geotech. Geoenv. Eng.*, 126(11), 1015-1025.

Andrus, R.D., Paramanthan, P., Ellis, B.S., Zhang, J., and Juang, C.H. [2004]. "Comparing Liquefaction Evaluation Methods Using Penetration-V_s Relationships," *Soil Dynamics and Earthquake Engineering*, 24, 713-721.

Baldi, G., Bellotti, R., Ghionna, V., Jamiolkowski, M. and Pasqualini, E. [1981]. "Cone Resistance in Dry Normally and Overconsolidated Sands," *Proceedings of GED Session on Cone Penetration Testing and Experience* (Norris and Holtz, eds.), ASCE National Convention, St. Louis, Missouri, October, pp. 145-177.

Bierschwale, J.G., and Stokoe II, K.H. [1984]. "Analytical Evaluation of Liquefaction Potential of Sands Subjected to the 1981 Westmorland Earthquake," *Geotechnical Engng. Rep. GR-84-15,* Civil Engineering Dept., U. of Texas, Austin.

Dobry, R., Stokoe II, K.H., Ladd, R.S., and Youd, T.L. [1981]. "Liquefaction Susceptibility from S-wave Velocity," *Proceedings ASCE Nat. Convention, In Situ Tests to Evaluate Liquefaction Susceptibility,* ASCE, New York.

Dobry, R., Ladd, R.S., Yokel, F.Y., Chung, R.M., and Powell, D. [1982]. "Prediction of Pore Water Pressure Buildup and Liquefaction of Sands During Earthquakes by the Cyclic Strain Method," *NBS Build. Sci. Ser. 138,* National Bureau of Standards, Gaithesburg, Maryland.

Finn, W.D.L. [1981]. "Liquefaction Potential: Developments Since 1976," *Proc. Intl. Conf. On Recent Advances in Geotechnical Earthquake Engineering and Soil Dynamics,* Vol. II, pp. 655-681.

Finn, W.D.L., Bransby, P.L., and Pickering, D.J. [1970]. "Effect of Strain History on Liquefaction of Sand," *J. of the Soil Mechanics and Foundations Div.*, ASCE, Vol. 96, No. SM6, 1917-1934.

Hardin, B.O. [1978]. "The Nature of Stress-Strain Behavior for Soils," *Proc. ASCE Geotech. Engng. Div. Specialty Conf. on Earthquake Engineering. And Soil Dynamics,* ASCE, New York, Vol. 1, pp. 3-90.

Hardin, B.O., and Drnevich, V.P. [1972]. "Shear Modulus and Damping in Sands, I, Measurement and Parameter Effects," *Tech. Rept. No. UKY 26-70-CE1,* U. of Kentucky, College of Engng., Soil Mechanics Series No. 1, Lexington, KY.

Idriss, I. M., and Boulanger, R. W. [2004]. "Semi-empirical Procedures for Evaluating Liquefaction Potential during Earthquakes." *Proc. 3rd Intl. Conf. on Earthquake Geotechnical Engineering* (D. Doolin, A. Kammerer, T. Nogami, R.B. Seed, and I. Towhata, eds.), U. of California, Berkeley, Vol. 1, 32-56.

Idriss, I.M, and Boulanger, R.W. [2008]. "Soil Liquefaction During Earthquakes," *Monograph MNO-12*, Earthquake Engineering Research Institute. Oakland, CA.

Lunne, T. and Kleven, A. [1981]. "Role of CPT in North Sea Foundation Engineering," *Proceedings of GED Session on Cone Penetration Testing and Experience* (Norris and Holtz, eds.), ASCE National Convention, St. Louis, Missouri, October, pp.76-107.

Robertson, P.K., Woeller, D.J., and Finn, W.D.L. [1992]. "Seismic CPT for Evaluating Liquefaction Potential," *Canadian Geotechnical J.,* 29:686-695.

Robertson, P.K., and Wride, C.E. [1998]. "Evaluating Cyclic Liquefaction Potential Using the Cone Penetration Test," *Canadian Geotechnical J*., 35(3), 442-459.

Schmertmann, J.H. [1973]. Discussion of "The Standard Penetration Test," by V.F.B. de Mello, *Proc. 4th Panamerican Conf. on Soil Mechanics and Foundation Engineering, San Juan, Puerto Rico, Vol. 3, pp. 90-98.*

Schmertmann, J.H. [1978]. "Cone Penetration Test Performance and Design," U.S. Department of Transportation, FHWA-TS-78-209.

Seed, H. B. [1979]. "Soil Liquefaction and Cyclic Mobility Evaluation for Level Ground During Earthquakes," *ASCE J. Geotechnical Engineering Div*., 105(GT2):201-255, February.

Seed, H.B. and Idriss, I.M. [1971]. "Simplified Procedure for Evaluating Soil Liquefaction Potential," *ASCE J. Geotech. Eng. Div.*, 97(9), 1249-1273, September.

Sharp, M.K. [1999]. "Development of Centrifuge Based Prediction Charts for Liquefaction and Lateral Spreading from Cone Penetration Testing", PhD thesis, Rensselaer Polytechnic Institute, Troy, N.Y.

Stokoe, II, K.H., Lee, S.H.H., and Knox, D.P. [1985]. "Shear Moduli Measurements Under True Triaxial Stresses," *Proc. Adv. In the Art of Testing Soil Under Cyclic Conditions,* ASCE, New York, 166-185.

Youd, T. L., and T. N. Craven [1975]. "Lateral Stress in Sands During Cyclic Loading," *ASCE J. Geotech. Eng. Div*., 101(GT2):217-221, February.

Youd, T. L., I. M. Idriss, R. D. Andrus, I. Arango, G. Castro, J. T. Christian, R. Dobry, W. D. L. Finn, L. F. Harder, Jr., M. E. Hynes, K. Ishihara, J. P. Koester, S. C. Liao, W. F. Marcuson III, G. R. Martin, J. K. Mitchell, Y. Moriwaki, M. S. Power, P. K. Robertson, R. B. Seed, and K. H. Stokoe II [2001]. "Liquefaction Resistance of Soils: Summary Report from the 1996 NCEER and 1998 NCEER/NSF Workshops on Evaluation of Liquefaction Resistance of Soils," *ASCE J. Geotech. and Geoenv. Eng.*, 127 (10):817-833, October.